J Ther Eng, Vol. 10, No. 6, pp. 1480−1493, November, 2024

Journal of Thermal Engineering
Web page info: https://jten.yildiz.edu.tr
DOI: 10.14744/thermal.0000889

Research Article

Investigations on the pyrolysis behavior of *Sapindus mukorossi* based on kinetic and thermodynamic parameters

Karunakarareddy LOMADA[1], Suraj POYILIL[1], Arun PALATEL[1,*], Muraleedharan CHANDRASEKHARAN[1]

[1]*Department of Mechanical Engineering, National Institute of Technology Calicut, Kozhikode, 673601, India*

ARTICLE INFO

Article history
Received: 09 September 2023
Revised: 01 February 2024
Accepted: 10 February 2024

Keywords:
Biomass; Iso-Conversional Methods; Model-Free Methods; Pyrolysis; Reaction Mechanism; *Sapindus Mukorossi*

ABSTRACT

Sapindus mukorossi (SM) is a fast-growing deciduous tree found extensively in tropical and sub-tropical regions of Asia. The conversion of SM seed shell (left over after extracting the pulp and kernal) to value added products through pyrolysis needs in-depth knowledge about its thermal degradation behavior. The present work studies the physicochemical properties, pyrolysis behavior, and kinetics of this less explored biomass feedstock for thermochemical conversion. The elemental composition, gross composition and higher heating value (HHV) of the SM shell is found to determine its energy potential. The kinetics of the pyrolysis reaction influence the breakdown of solid biomass into final products. Thermogravimetric analysis (TGA), wherein the sample is heated at various heating rates (5, 10, 20 °C/min) at inert condition reveals the thermal degradation profile of SM seed shell. Three important isoconversional model-free techniques, notably Friedman, Ozawa-Flynn-Wall (OFW), and Kissinger-Akahira-Sunose (KAS) approaches, are employed to obtain the kinetic triplet data, the thermodynamic parameters are also determined. The C, H, N, S and O content of the SM shell was found to be 39.82%, 4.64%, 0.64%, 0.64% and 54.26% respectively. The SM seed shell had a volatile matter, fixed carbon and HHV of 68.5%, 20.9% and 16.6 MJ/kg respectively which revealed its energy potential for thermochemical conversion. From the TGA curve, the maximum thermal degradation was observed between 200 °C and 500 °C. The values of average activation energy determined using models Friedman, OFW and KAS are 152.28 kJ mol^{-1}, 140.05 kJ mol^{-1} and 138.14 kJ mol^{-1}, respectively. The frequency factor was found to vary widely between 10^3 and 10^{15}. The variation in activation energy and frequency factor as the conversion progresses indicated complicated processes during the thermal deterioration of SM. The biomass degradation occurs by diffusion and nucleation mechanisms when the conversion value is between 0.2 and 0.5, and for conversion values in the range of 0.6–0.8, the degradation occurs by diffusion mechanisms. The physicochemical characteristics of SM are found to be comparable with that of the commonly available biomasses. The detailed investigations presented in this paper have clearly demonstrated the viability of SM seed shell as a viable feedstock for the pyrolysis process.

Cite this article as: Lomada K, Poyilil S, Palatel A, Chandrasekharan M. Investigations on the pyrolysis behavior of Sapindus mukorossi based on kinetic and thermodynamic parameters. J Ther Eng 2024;10(6):1480−1493.

***Corresponding author.**
*E-mail address: arun.p@nitc.ac.in

This paper was recommended for publication in revised form by Editor-in-Chief Ahmet Selim Dalkılıç

INTRODUCTION

Biomass, an abundantly available energy resource, is being viewed as an effective replacement for fossil fuels. The carbon neutrality of biomass makes it a prime short-cycle carbon source for meeting future energy needs. Biomass resources provide energy security and support the rural economy, especially in developing countries. In India, almost 32 percent of the primary energy usage of the nation is still derived from biomass [1]. In the coming years, the demand for energy is anticipated to increase at a rate of about 4.8% annually. Biomass is a feasible substitute for fossil fuels when employed for energy production in rural areas. The share of total energy consumption in rural areas of developing countries met by biomass are: India (47%), Pakistan (27%), Brazil (25%), and China (13%) [2]. According to an estimate, the world's population dependency on biomass as a primary energy source will be 15-50% by the year 2050 [3]. Biomass is an easily available, economical, renewable source of energy [4]. Biomass includes residues from agriculture (like rice husk, wheat straw, etc.), oil and food processing industries (like sugarcane bagasse, de-oiled cakes, etc.), forest residues (like wood chips, leaves, and seeds), solid waste (vegetable waste), and sludge from wastewater treatment plants that have reasonable bioenergy content [5, 6]. In addition to being a cost-effective and sustainable source of energy, biomass energy also provides a solution for the disposal of solid waste [7]. The primary conversion methods for biomass-based feedstock into fuel include thermochemical, biochemical, and mechanical processes. The lower cost and higher efficiency of thermochemical techniques make the process prominent over biochemical [8]. Liquefaction, pyrolysis, gasification, and combustion are the widely adopted thermochemical techniques. Feedstock properties, reactor design, and reaction conditions can influence the efficiency of the thermochemical conversion process [9]. The pyrolysis process helps in thermal cracking of biomass into useful chemicals, biofuels, and absorbent biochar, which usually takes place in an inert atmosphere at a temperature of 400-700 °C [4]. The process involves complex chemical reactions, heat, and mass transfer phenomena happening inside. The characteristics and nature of the products depend on the type of biomass, heating rate, and type of reactor [10]. It was reported that once the kinetics and thermodynamics parameters are established, it is easy to examine the viability of feedstock, scale up reactors, run them, and optimize them [11–14].

About 50% of the world's biomass is estimated to come from lignocellulosic biomass, the global production of lignocellulosic biomass accounts for approximately 181.5 billion [15]. *Sapindus mukorossi* is a deciduous tree, commonly known as 'Areetha' or Indian soap berry. The generic name is derived from the Latin words 'sapo' and 'indicus.' The seed of *Sapindus mukorossi* contains 23% of oil [16]. The kernel of soap nut seed was identified as a potential feedstock for biodiesel production [17]. *SM* is cultivated as an ornamental plant in the northern part of India. The pulp of the soap nut contains a high level of natural foaming agents [18, 19]. Due to the abundance of this feedstock, studies on its potential application as a biofuel have been considered. Knowledge of reaction kinetics is vital for analyzing processes aimed at an efficient transformation of solid biomass into useful energy. The purpose of the kinetic analysis is to interpret the obtained kinetic triplet data experimentally [20]. The kinetic triplet data consists of activation energy, frequency factor, and differential (or) integral form of the model [21]. Activation energy is associated with the energy barrier; frequency of vibrations of activated complex is associated with the frequency factor and differential (or) integral form of a model with the reaction mechanism [22, 23]. During the thermal decomposition of materials, kinetic parameters obtained from the reaction are essential for generating accurate data to understand the reaction process and optimizing process parameters. Thermogravimetric methods are proven to be helpful for the analysis of pyrolysis reaction kinetics for a better understanding of the thermal decomposition of biomass [24]. It is possible to assess the pyrolysis kinetic behavior of a feedstock using iso-conversional and model fitting techniques. Both of these methods are applicable for isothermal and non-isothermal operating conditions [25, 26]. Single step, parallel reaction, pseudo components, and distributed activation energy models (DAEM) are the TGA-dependent models used to evaluate the feedstock pyrolysis kinetic behavior [27]. Patnaik et al. [28] investigated the thermal degradation of corn starch-based plates and used TGA data at different temperatures to determine the kinetic parameters. The experimental data from TGA obtained at different heating rates gives insight into the conversion mechanism and reaction kinetics [29–31].

One of the crucial steps in model fitting procedures is choosing a suitable kinetic model. Broström et al. [32] investigated the pyrolysis kinetics of Norway spruce based on a multi-pseudo component kinetic model. Tapasvi et al. [33] analyzed the pyrolysis kinetics with a more detailed and complex DAEM. Prior knowledge of the reaction mechanism is required for model-fitting methods [25]. The type of reaction and the morphology of the reactants are useful parameters for identifying the reaction model. The description of complex kinetics by multi-step reaction models uses model-fitting methods, but some nontrivial problems are encountered in applying these methods [34]. The kinetics of solid-state reaction processes are often described with iso-conversional methods. The benefit of using the iso-conversional method is that a complicated, multi-step process is treated as a single-step process. Ben Abdallah et al. [4] reported the wide acceptance of the iso-conversional method in investigating the chemical kinetics of biomass. The iso-conversional method had become more popularized after the recommendation of International Confederation for Thermal Analysis and Calorimetry (ICTAC) [34, 35]. Many computational techniques were created adopting

the iso-conversional concept, with differential and integral being the two categories into which they can be classified [34, 36]. The Friedman, Ozawa-Flynn-Wall (OFW), Kissinger-Akahira-Sunose (KAS), and Starink methods are widely used non isothermal, iso-conversional model free approaches for a conversion range of 0.1-0.9 for calculating the kinetic parameters [37–39]. Friedman's method comes under the differential category, which employs instantaneous rate values and is sensitive to experimental noise, leading to numerical instability. Integral methods include KAS and OFW, which are developed approximating the temperature integral based on Doyle's approximations [40]. Singh et al. [41] studied the pyrolysis behavior of garlic husk and determined its kinetic parameters using Starink, OFW, and KAS methods. The thermodynamic parameters like enthalpy, entropy and Gibbs free energy were also estimated. Komandur et al. [39] determined the activation energy and pre-exponential factor of Mesua ferrea L, which is a non-edible oil seed. The experimental data of TGA was determined at different heating rates (5, 10, 20 and 40 °C/min). The average activation energy of Aegle mamelos L. and Phoenix dacylifera seed was found by Pal et al. [38]. The activation energy for Phoenix dacylifera seed was 173.75, 172.94, and 170.71 kJ/mol as calculated by KAS, FWO, and Starink model; for Aegle mamelos L., it was 170.26, 167.24, and 164.80 kJ/mol. The activation energies of the biomass vary due to the physical and chemical composition differences of different biomass. The kinetic parameters, including activation energy, were also determined in a number of different investigations by use of the Friedman, OFW, and KAS techniques [20, 42, 43]. The analysis of experimental data using integral methods gives activation energy by averaging over the whole conversion range. Inconsistency between the activation parameters derived from isothermal and non-isothermal experiments is attributed to the difference in the averaging process followed for integral and differential methods. On comparing the ideal master plot and experimental master plot, the reaction mechanism was also evaluated [44]. Based on master plot analysis, it was determined that the reaction model pertaining to garlic husk biomass was matching with a second order reaction [41].

The thermal degradation profile of biomass involves complex reaction mechanisms with varying activation energy. In the available literature, investigations on the feasibility of SM seed shell as a potential feedstock for pyrolysis and gasification have not been found. A detailed study regarding thermal decomposition, pyrolysis kinetics, and its thermodynamics needs to be explored. Hence, the present study concentrates on determining the pyrolysis kinetic behavior of SM seed shell with the help of TGA in non-isothermal conditions using the iso-conversional methods of KAS, OFW, and Friedman and to compare with solid state reaction models by generating master plot.

MATERIALS AND METHODS

Procurement and Preparation of Sample

The species *Sapindus mukorossi (SM)* is a member of the kingdom Plantae and the family Sapindaceae. It belongs to the Sapindus genus. The tree is a rather large deciduous tree with leathery leaves. It grows to a height of 15 to 20 metres and a circumference of 1.8 meters [45]. *Sapindus mukorossi* seeds are procured from regional markets, exposed to the sun for 48 hours, and then sealed in a bag. After removing the kernel from SM seeds, the seed shells are dried in an oven using hot air before being ground into tiny pieces with a mean particle diameter of less than 1.0 mm. The processes involved are shown in Figure 1.

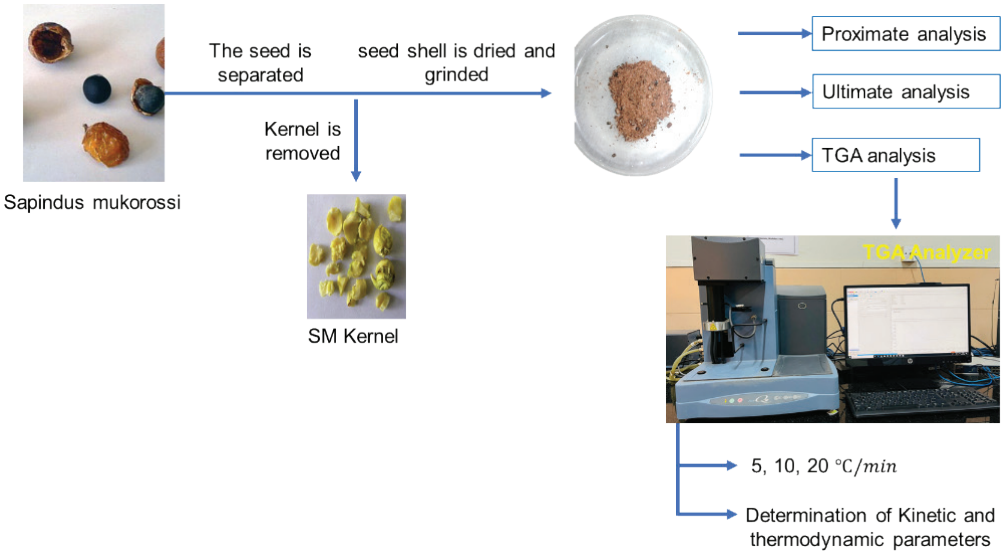

Figure 1. Sample preparation and analysis.

Proximate and Ultimate Analyses

The proximate analysis details the biomass sample's moisture content (MC), volatile matter (VM), fixed carbon (FC), and ash (A). ASTM D 2016-74 is followed for analyzing moisture content. The SM seed shell sample weighing 1 g is placed in a silica crucible and then heated for 1 hour at 105 ± 5 °C in a muffle furnace. The Initial and final weights of the sample are observed, and Eqn. (1) is used to determine the moisture content. The volatile matter and ash content percentages are calculated according to ASTM E-872-82 and ASTM D 1102-84, respectively. The same biomass sample used for moisture analysis is placed inside a muffle furnace and maintained at 950 °C temperature for 7 minutes, and the observed difference in weight loss gives the percentage of volatile matter and is calculated using Eqn. (2). The furnace temperature is then adjusted to 525 °C and the sample is maintained at that temperature for a duration of 4 hours. The final weight of the sample left in the crucible after the analysis is used to determine the amount of ash content present in the sample, using Eqn. (4).

$$Moisture\ Content,\ MC\ (\%) = \frac{w-b}{w} \tag{1}$$

$$Volatile\ Matter, VM\ (\%) = \frac{b-c}{w} \tag{2}$$

$$Ash\ content, A\ (\%) = \frac{a}{w} \tag{3}$$

$$Fixed\ carbon, FC\ (\%) = 100 - [MC\ (\%) + VM\ (\%) + Ash\ content\ (\%)] \tag{4}$$

where w is the weight of the sample taken for proximate analysis, b is the sample weight recorded after drying, c is the sample weight recorded after releasing volatile matter, and a is the weight of the ash left in the crucible. The ultimate analysis provides the elemental composition (in percentage). The percentages of C, H, N, and S in the sample are estimated using a Perkin-Elmer Elemental Analyzer at the Sophisticated Analytical Instruments Facility (SAIF), STIC, Kochi, India. Oxygen content is calculated by subtracting the sum of C, H, N, and S from the total. The HHV or gross calorific value of biomass indicates the amount of heat energy liberated per kilogram of biomass, taking the latent heat of vaporization of water into account.

Thermogravimetric Analysis

Pyrolysis is a thermal degradation process in which the feedstock is heated in the range of 400 – 700 °C under an inert atmosphere [46]. The thermal degradation of biomass is dependent on the percentage of cellulose, hemicellulose, and lignin present in the sample. The effective pyrolysis temperature of the SM seeds can be determined by TGA, which is carried out using the instrument TGAQ50 (TA instruments). Approximately a mass of 5-10 mg of SM seed is taken in a pan and heated to a temperature of 900 °C, and a one-minute residence time is allowed at that temperature. TGA is performed in the current investigation at three different heating rates (5, 10, and 20 °C min^{-1}). The plot between thermogravimetric weight loss (%) and temperature (°C) provides information about the temperature range where maximum thermal degradation of biomass takes place.

Determination of Kinetic Parameters

With the help of TG analysis, the various kinetic characteristics of the SM seed shell, including activation energy and frequency factor, are to be determined. The kinetic parameters are essential during the pyrolysis of biomass, where several reactions occur simultaneously, involving complex reaction mechanisms. The global reaction can be represented as:

$$Biomass\ k \rightarrow Volatiles + Char$$

Where k represents the reaction rate constant and the volatiles in the reaction account for different gases and tar formed during the process. The degree of conversion (α) can be used to express the reaction rate of the pyrolysis process, as given in Eqn. (5).

$$\frac{m_i - m}{m_i - m_f} = \alpha \tag{5}$$

where $m_i - m\ and\ m_i - m_f$ are current mass change and total mass change, respectively. The rate of reaction can be represented as given in Eqn. (6).

$$\frac{d\alpha}{dt} = k(T) f(\alpha) \tag{6}$$

where k(T) is the reaction rate constant as a function of temperature and f(α) is the differential form of the reaction model. Eqn. (7) gives the relationship between the activation energy and reaction rate constant.

$$k\ (T) = Ae^{\left(\frac{-E}{RT}\right)} \tag{7}$$

Here A, E, R, and T are the frequency factor, activation energy, universal gas constant, and temperature, respectively. The rate of heating (δ) is expressed in Eqn. (8)

$$\delta = \frac{dT}{dt} = \frac{dT}{d\alpha}\frac{d\alpha}{dt} \tag{8}$$

$$g(\alpha) = \int_0^{\alpha} \frac{d\alpha}{f(\alpha)} = \frac{AE}{\delta R} u(\alpha) \tag{9}$$

g(α) and f(α) functions in Eqn. 9 represent the integral and differential functions of the reaction mechanism and $\alpha = \frac{E}{RT}$. Since there is no exact solution for the temperature integral function $u(\alpha)$, the solution is found through approximation methods.

Kissenger-Akahira-Sunose (KAS)

The integral reaction method KAS is used to predict the kinetic behavior of biomass in the pyrolysis process, and the corresponding relation is given in Eqn. (10).

$$ln\left(\frac{\delta}{T^2}\right) = ln\left[\frac{AR}{Eg(\alpha)}\right] - \frac{E}{RT} \quad (10)$$

By plotting the curve between $ln\left(\frac{\delta}{T^2}\right)$ and (1/T) at different heating rates, the slope of the curve gives activation energy *E*, and the intercept of the curve gives the frequency factor.

Ozawa-Flynn-Wall (OFW)

OFW is one of the model-free methods used to calculate the kinetic parameters. The value of the function $u(x)$ is approximated by Doyle's method using the first three terms of the Schlomilch series expansion and the following approximation of temperature integral is obtained [47].

$$\log (u(\alpha)) = -2.315 - 0.457\,\alpha \quad (11)$$

Substitution of approximated functional value and rearrangement of terms in Eqn. (9) gives:

$$\ln(\delta) = \ln\left[\frac{AE}{g(\alpha)R}\right] - 2.315 - 0.457\alpha \quad (12)$$

The activation energy and frequency factor can be calculated from the slope and intercept of a plot between ln(δ) and 1/T for various heating rates.

Friedman method

It is one of the iso-conversional methods and the generalized form of a differential method that can be obtained from Eqns. (8) and (9):

$$ln\left(\frac{d\alpha}{dt}\right) = \frac{-E}{RT} + ln\ (A\,f(\alpha)^n) \quad (13)$$

Where *n* is the order of a reaction.

According to Friedman, the conversion function term $f(\alpha)^n$ is constant, and the biomass degradation depends only on the mass-loss rate and is independent of temperature [48]. A graph plotted between $ln\left(\frac{d\alpha}{dt}\right)$ and 1/T gives the slope and intercept of the curve for evaluating activation energy and frequency factor of the pyrolysis reaction, respectively.

Thermodynamic Analysis

The thermal stability of biomass is correlated with thermodynamic parameters such as a change in enthalpy, entropy, and Gibbs free energy. The endothermic (or exothermic) nature of the reaction process, system reactivity, and thermodynamic equilibrium are indicated by enthalpy change, entropy change, and Gibbs free energy, respectively. The Eqns. (14-17) are used to calculate the frequency factor or pre-exponential factor (A), change in enthalpy (H), change in Gibbs free energy (G), and change in entropy (S) of the degradation process [49].

$$A = \frac{\delta E e^{\left(\frac{E}{RT_m}\right)}}{RT_m^2} \quad (14)$$

$$\Delta H = E - RT \quad (15)$$

$$\Delta G = E + RT_m\left[ln\left(\frac{K_B T_m}{hA}\right)\right] \quad (16)$$

$$\Delta S = \frac{\Delta H - \Delta G}{T_m} \quad (17)$$

Where T_m: temperature (K) at maximum decomposition, K_B: Boltzmann constant, h: Planck's constant, δ: heating rate, E: activation energy, R: gas constant

Reaction Mechanism (Z-master Plot)

According to Criado et al. [50], the thermal degradation rate of solid material can be expressed as:

$$\frac{d\alpha}{dt} = Ae^{\left(\frac{-E}{RT}\right)} f(\alpha) \quad (18)$$

Combining integral and differential forms of the particular reaction model gives the Z(α) curve. The Z (curve), also referred to as a master chart, is a theoretical curve that depends on the reaction's kinetic model but is unaffected by the activation energy or pre-exponential factor.

$$Z(\alpha) = f(\alpha) \times g(\alpha) = \frac{d\alpha}{\delta dt} e^{\alpha} \int_0^T e^{-\alpha} dT \quad (19)$$

The experimental plots and the generating equation for theoretical master plots are equated in Eqn (19). The fourth-order rational formula of the Senum-Yang approximation was used to find an approximation of the temperature integral. The error obtained for α>20 is less than 10^{-5} % [51]. The theoretical curve can be compared with an experimental curve to identify the nature of the reaction mechanism. The equations of different physical models are listed in Table 1.

RESULTS AND DISCUSSION

SM Seed Shell Characterization

The physicochemical characterization results of the SM seed shell are given in Table 2. According to the proximate analysis, the biomass contains a volatile matter content of 68.5%, an ash content of 1.1%, a moisture content of 9.5%, and a fixed carbon content of 20.9%.

More volatile matter suggests the easiness of ignition during combustion. A high amount of volatile matter could yield a higher liquid during pyrolysis [27]. The lower percentage of ash indicates that the feedstock is expected to have a better calorific value, whereas higher ash content reduces the effectiveness of the pyrolysis process by acting as a heat sink. A dry ash-free basis is used for ultimate analysis. It reveals the percentage composition of carbon (C),

Table 1. Differential and integral equations for different solid-state decomposition processes [52]

Symbol	$f(\alpha) = \left(\frac{1}{k}\right)\left(\frac{d\alpha}{dt}\right)$	$g(\alpha) = kt$
Geometrical contraction model		
R1	1	α
R2	$2(1-\alpha)^{1/2}$	$1-(1-\alpha)^{1/2}$
R3	$3(1-\alpha)^{2/3}$	$1-(1-\alpha)^{1/3}$
Diffusional model		
D1	$\frac{1}{2\alpha}$	α^2
D2	$[-ln(1-\alpha)]-1$	$(1-\alpha)\,ln(1-\alpha)+\alpha$
D3	$\frac{3}{2}(1-\alpha)^{\frac{2}{3}}\left[1-(1-\alpha)^{\frac{1}{3}}\right]^{-1}$	$\left[1-(1-\alpha)^{\frac{1}{3}}\right]^2$
D4	$\frac{3}{2}\left[(1-\alpha)^{\frac{1}{3}}-1\right]^{-1}$	$1-\left(\frac{2}{3}\right)\alpha-(1-\alpha)^{2/3}$
Nucleation model		
A1.5	$\frac{3}{2}(1-\alpha)[-ln\,ln(1-\alpha)]^{\frac{1}{3}b}$	$[-ln\,(1-\alpha)]^{\frac{2}{3}}$
A2	$2(1-\alpha)[-ln\,(1-\alpha)]^{\frac{1}{2}}$	$[-ln\,(1-\alpha)]^{\frac{1}{2}}$
A3	$3(1-\alpha)[-ln\,(1-\alpha)]^{\frac{2}{3}}$	$[-ln\,(1-\alpha)]^{\frac{1}{3}}$
A4	$4(1-\alpha)[-ln\,(1-\alpha)]^{\frac{3}{4}}$	$[-ln\,(1-\alpha)]^{\frac{1}{4}}$
A4/5	$\frac{4}{5}(1-\alpha)[-ln\,(1-\alpha)]^{-\frac{1}{4}}$	$[-ln\,(1-\alpha)]^{\frac{5}{4}}$
A5/6	$\frac{5}{6}(1-\alpha)[-ln\,(1-\alpha)]^{-\frac{1}{5}}$	$[-ln\,(1-\alpha)]^{\frac{6}{5}}$
Order based model		
F1	$1-\alpha$	$-[-ln\,(1-\alpha)]$
F1.5	$(1-\alpha)^{\frac{3}{2}}$	$2[(1-\alpha)^{-\frac{1}{2}}-1]$
F2	$(1-\alpha)^2$	$[(1-\alpha)^{-1}-1]$
F3	$(1-\alpha)^3$	$\frac{[(1-\alpha)^{-2}-1]}{2}$
F4	$(1-\alpha)^4$	$\frac{[(1-\alpha)^{-3}-1]}{3}$
Power law model		
P1.5	$\frac{3}{2}\alpha^{\frac{1}{3}}$	$\alpha^{\frac{2}{3}}$
P2	$2\alpha^{\frac{1}{2}}$	$\alpha^{\frac{1}{2}}$
P3	$3\alpha^{\frac{2}{3}}$	$\alpha^{\frac{1}{3}}$
P4	$4\alpha^{\frac{3}{4}}$	$\alpha^{\frac{1}{4}}$

Table 2. Physicochemical characterization of SM seed shell

Type of analysis	Standard	SM seed shell
Proximate Analysis (wt. %)[a]		
Moisture	ASTM D 2016-74	9.5
Ash	ASTM D 1102-84	1.1
Volatile Matter	ASTM E 872-82	68.5
Fixed Carbon	Calculation	20.9
Ultimate Analysis (wt.%)[b]		
C		39.82
H		4.64
N		0.64
S		0.64
O	By difference	54.26
H/C molar ratio	Calculation	1.38
O/C molar ratio	Calculation	1.02
Molecular formula	Calculation	$CH_{1.38}O_{1.02}$
Heating value (MJ/kg)		
HHV	ASTM D 2015-85	16.06

[a]Weight percentage on a dry basis [b]on dry ash-free basis

hydrogen (H), nitrogen (N), and sulphur (S) as 39.82%, 4.64%, 0.64% and 0.64%, respectively. The oxygen content is determined by difference and found to be 54.26%. The HHV of the SM seed shell is found to be 16.06 MJ/kg using a bomb calorimeter.

Thermogravimetric Analysis of SM Seed Shell

The TGA and Differential Thermogravimetric analysis (DTG) profiles of SM seed shells are shown in Figure 2 and 3, respectively. Thermograph demonstrates that biomass degraded in stages at three distinct heating rates (5, 10, and 20 °C min^{-1}). TGA data of at least three heating rates are required for the iso-conversional analyses [29]. The percentage reduction in the weight of the biomass sample with temperature is obtained from the TGA. Figure 2 shows that the removal of moisture and light organic components occurs within 200 °C, and it is known as the drying stage, which is almost the same at all heating rates [53]. Further, maximum degradation occurs in the active pyrolytic stage (200-500 °C) due to an increased pyrolysis rate. In this stage, cellulose and hemicellulose are degraded, resulting in the release of volatiles. During the passive pyrolytic stage (>500 °C), the biomass degradation rate is lower due to the complex molecular structure of lignin. The DTG profile of the SM seed shell confirmed that biomass degradation took place in three zones, as shown in Figure 3. In the first zone, with the evaporation of water molecules at a temperature below 100 °C first peak of DTG is observed. In the temperature range 100-150 °C, complete evaporation of moisture took place. The release of light volatile compounds is inferred at a temperature range of 150-250 °C. In the second zone, the peak found at 248 °C and 320 °C confirms the decomposition initiation of hemicellulose and cellulose, respectively. A slower rate of lignin decomposition at the last stage of the process, which favors the development of char, can be seen in the third zone from DTG profiles at a temperature of more than 500 °C. In most of the reported TGA results, different biomasses like agro-waste, coffee husk, sugarcane bagasse, bean pod, corn stover, etc. [7, 54, 55], similar degradation profiles are obtained.

DTG profiles at various heating rates show that the peak of DTG curves is shifted into the area of higher temperature with an increase in heating rate from 5 to 20 °C min^{-1}.

Due to the weak thermal conductivity of the biomass sample, there is a temperature gradient that increases with the heating rate and causes a change in the degradation temperatures and a limited amount of heat transfer from the sample to the surface of the furnace pan [56].

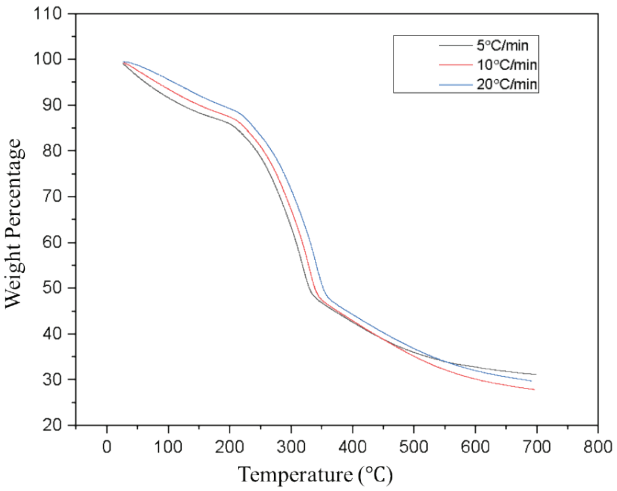

Figure 2. SM seed shell TG profile at different heating rates.

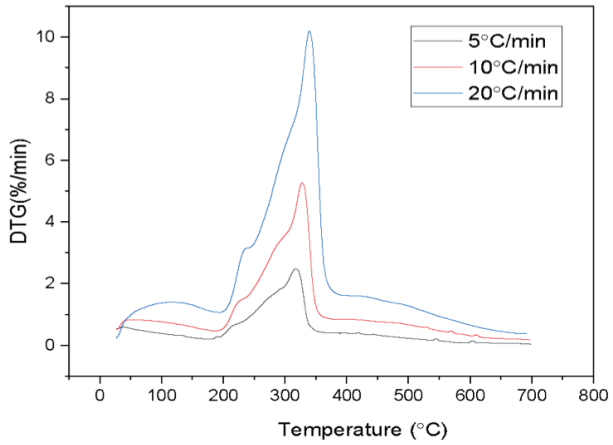

Figure 3. SM seed shell DTG profile at different heating rates.

Table 3. Comparison of activation energies of SM seed shell with other biomasses

Biomass	Heating rate (°C min^{-1})	KAS (kJ mol^{-1})	OFW (kJ mol^{-1})	Friedman (kJ mol^{-1})	References
Sapindus mukorossi	5,10 and 20	138.14	140.05	152.28	Present study
Sawdust (Pine)	5,10,15,20 and 25	171.66	179.29	168.58	[27]
Sawdust (Sal)	5,10,15,20 and 25	148.44	156.58	181.53	[27]
Areca nut husk	5,10,15,20 and 25	171.24	179.47	181.61	[27]
Madhuca longifolia	5-25	114.14	150.21	123.11	[27]
Sugarcane bagasse	5,7.5,10	52.31	61.71	121.72	[57]
Rice husks	5-20	-	169.00	182.20	[58]
Cacao shells	5-20	-	145.60	133.70	[58]

Pyrolysis Kinetics of SM Seed Shell

Iso-conversional methods like KAS, OFW, and Friedman are used for the kinetic analysis of SM seed shell. The slower the rate of reaction, the higher the activation energy required. Pyrolysis parameters like activation energy and frequency factor are obtained by curve-fitting the conversion value against temperature data into linear equation form. The slope and intercept of the linear equation give activation energy and frequency factor, respectively. Using KAS, OFW, and Friedman methods, the average activation energies obtained are 138.14 kJ mol^{-1}, 140.05 kJ mol^{-1}, and 152.28 kJ mol^{-1}, respectively. Table 3 compares the average activation energy for the SM seed shell, which was determined in the present study using model-free approaches, with that of other biomasses.

Figure 4 shows the ordinates of the iso-conversional methods (KAS, OFW, and Friedman) against 1/T for fractional conversion ranges of 0.1-0.8 at heating rates of 5, 10, and 20 °C/min. From Figure 4(c), the non-parallel nature of the plot using Friedman's method revealed the complex mechanism of biomass degradation [59]. Table 4 shows the coefficient of determination (R^2) value of the linear equation and the corresponding fractional conversion (α) value of the SM seed shell. For a fractional conversion range of 0.2-0.5, the perfect linear relationships ($R^2 \geq 0.99$) indicate the accuracy of the kinetic data. The poor fitting of data ($R^2 < 0.99$) at a lower and higher conversion value indicates the nature of reactions is heterogeneous because of secondary reactions. The degradation of biomass at a higher conversion value was through the diffusion process [60]. The increase in the activation energy with the increase in the percentage conversion, as given in Table 4 indicates the influence of temperature and conversion ratio on the activation energy [61].

During the kinetic analysis of SM seed shell using model-free methods, poor coefficient of determination values were observed for conversion values above 0.8 which implies the inaccuracies of data, so it was not considered further for the analysis. In the present study, the values of average activation energy (E) obtained by two integral methods (KAS, OFW) are almost equal, as shown in Table 4. In contrast to the values obtained using the Friedman technique, the values from KAS and OFW were significantly different. The variations of activation energy with conversion value follow a similar trend (parallel in nature) for integral methods KAS and OFW, as shown in Figure 4 (a) and (b). The variation in activation energy differential, computed by Friedman's method as shown in Figure 4 (c), is more accurate than that obtained by integral methods. The higher R^2 values achieved for Friedman's technique indicate this. The combination of the integral and Friedman's differential methods was found to be more reliable in determining the appropriate activation energies of biomass [59]. The activation energy determined by KAS and OFW is found to be lower than the Friedman method. The activation energy determined by the Friedman method was reported to be accurate compared to the other two. This is because of the assumption of constant activation energy during the integration of Arrhenius equation for the derivation of OFW and KAS method. The activation energy, which varies throughout the reaction, is approximated as a constant in the temperature integral, which induces error [44, 62].

Thermodynamic Parameters

The activation energy estimated by the Friedman method is used for calculating relevant thermodynamic parameters. The thermodynamic analysis revealed that enthalpy change (ΔH) had a lower value during the initiation of the pyrolysis reaction and then reached a higher value as the reaction progressed. As the reaction progresses, the variation in ΔH indicates that the energy required to activate the remaining feedstock increases. Table 5 shows the thermodynamic parameters of the SM seed shell that are calculated using the activation energy obtained from the Friedman method for a heating rate of 10 °C min^{-1}. The R^2 value obtained by the Friedman method is high as compared to KAS and OFW. The frequency factor, one of the thermodynamic parameters, is calculated by Eqn. (14), and it is varied with a fractional conversion value (α) from 0.026×10^3 to 1.085×10^{15}. The average frequency factor is found to be 8.118×10^{19}. The frequency factor indicates the surface reaction. Assuming that the pyrolysis reactions

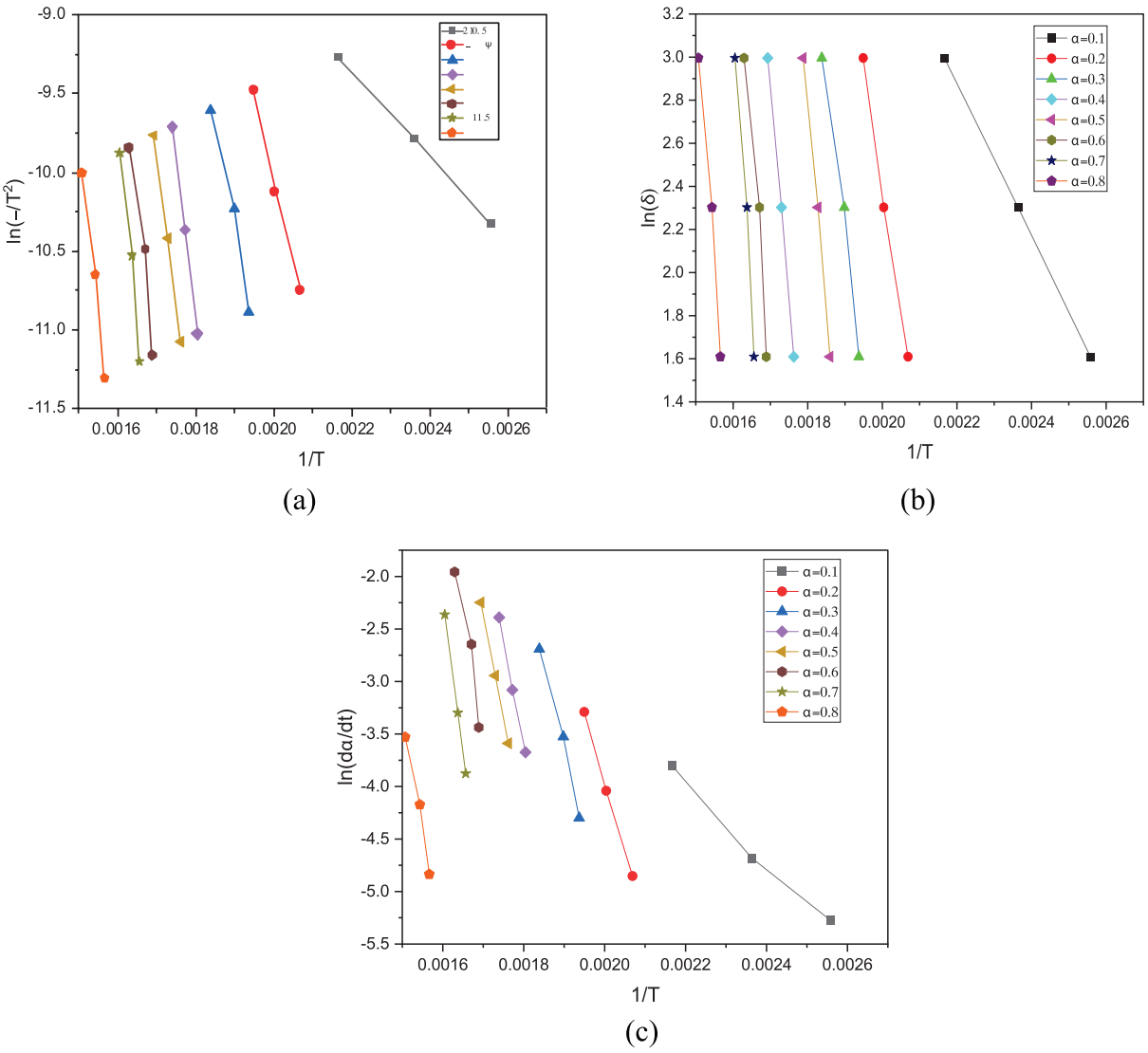

Figure 4. Decomposition plots of SM seed shell at different heating rates(a) KAS plot, (b) OFW plot, and (c) Friedman plot.

Table 4. Kinetic analysis data of SM seed shell using KAS, OFW, and Friedman model

α	KAS			OFW			Friedman		
	Slope	E ($kJmol^{-1}$)	R^2	Slope	E ($kJmol^{-1}$)	R^2	Slope	E ($kJmol^{-1}$)	R^2
0.1	2688.456	22.351	0.999	3539.99	27.976	0.999	3766.143	31.311	0.988
0.2	10536.341	87.599	0.997	11515.692	91.008	0.997	13089.274	108.824	0.999
0.3	12742.233	105.938	0.982	13784.458	108.939	0.985	16153.764	134.302	0.990
0.4	20197.118	167.918	0.999	21325.932	168.539	0.999	19752.016	164.218	0.996
0.5	18925.957	157.350	0.999	19896.126	157.239	0.998	19686.840	163.676	0.999
0.6	20727.626	172.329	0.943	22104.681	174.694	0.950	23388.282	194.450	0.931
0.7	25292.216	210.279	0.973	26534.648	209.704	0.976	29233.723	243.049	0.999
0.8	21815.079	181.370	0.982	23075.712	182.368	0.982	21462.528	178.439	0.982
Average activation energy									
138.14				**140.05**			**152.28**		

Table 5. Thermodynamic analysis of SM seed shell using Friedman model

α (Conversion)	Enthalpy ΔH (kJ mol^{-1})	Gibbs free energy ΔG (kJ mol^{-1})	Entropy ΔS (kJ mol^{-1} K^{-1})
0.1	27.795	164.979	-0.229
0.2	104.675	158.685	-0.090
0.3	129.922	157.639	-0.046
0.4	159.528	156.639	0.004
0.5	158.869	156.655	0.003
0.6	189.477	155.799	0.056
0.7	237.971	154.689	0.139
0.8	176.955	156.226	0.034
Average	**148.149**	**157.664**	**-0.129**

are independent of the surface area of the biomass sample, the lower frequency factor indicates a higher interaction between the molecules, and a higher frequency factor indicates a lower interaction [63].

The activation energy found using the Friedman method is used to find the average enthalpy change of the SM seed shell. The positive value of ΔH indicates the energy required for biomass decomposition. The enthalpy variation with fractional conversion value reveals the complex nature of biomass conversion. As the reaction progresses, the variation in ΔH indicates that the energy required to activate the remaining feedstock increases, and it also denotes that the conversion process is endothermic [24] The lower enthalpy value at the beginning denotes the lesser energy requirement to initiate the pyrolysis process [29]. The average ΔS value of -0.129 kJ mol^{-1} K^{-1} indicates the disorder of products formed by dissociation of bonds, and it is higher compared to the initial disorder of reactants. The negative and positive values of entropy with the increase in the conversion fraction indicate the complexity of the reaction [64]. The biomass sample had attained a state of thermodynamic equilibrium by undergoing a physical and chemical ageing process. During this situation, the reactivity of biomass sample is low, which increases the time of formation of the activated complex. If high activation entropy values are observed, it indicates that the biomass material is far from thermodynamic equilibrium, so system reactivity increases to produce the activated complex by reducing reaction time. ΔG value indicates reaction spontaneity, and the average value of ΔG for the SM seed shell is found to be 157.664 kJmol^{-1}. The positive value of ΔG indicates the non-spontaneous nature of the process [23].

Reaction Mechanism (Master Plot)

The master plot finds application in determining the reaction mechanism possible during the decomposition of solid fuels [65]. It depends on the kinetic model of a reaction and is independent of the activation energy and preexponential factor.

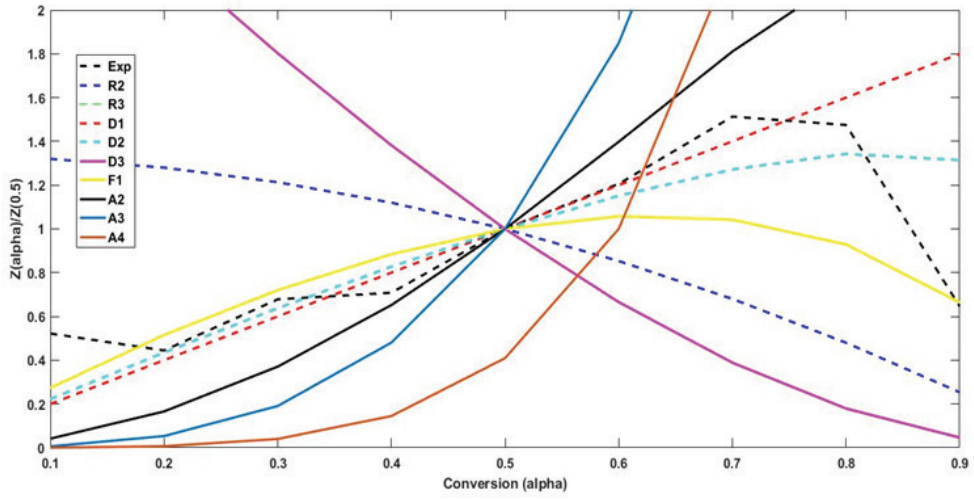

Figure 5. Master plot comparison of solid-state reaction models with an experimental model.

Figure 5 shows a comparison between the experimental and solid-state reaction models (Table 1) by the Z (α) master plot developed using MATLAB software. Irrespective of the biomass variant pyrolyzed, the normalized experimental $Z(\alpha)/Z(0.5)$ curve is poorly fitted with the theoretical curves of solid-state reaction models [58]. In Figure 5, R2 and R3 correspond to the geometrical contraction model, and D1, D2, and D3 correspond to the diffusional model. F1 represents the order-based model, whereas A2, A3, and A4 correspond to the nucleation model. The reaction mechanism is evaluated by considering the accuracy of fitting and similarities in shapes between curves obtained from the theoretical and experimental models [59]. In TGA analysis, the weight loss percentage of the biomass sample is represented in terms of the conversion value. The experimental curve resembles the diffusion model for a conversion value of 0.2 to 0.3 when the conversion value is varied from 0.1 to 0.9, as illustrated in Figure 5. For conversion values 0.3 to 0.4, shifting of the experimental curve is observed between solid-state reaction models. For the variation of conversion value from 0.4 to 0.5, the experimental curve follows the nucleation model, and for a variation from 0.6 to 0.8, the experimental curve follows the diffusion model as shown in the master plot. Comparison of DTG analysis with master plot indicates that the char formation takes place at a temperature above 500 °C. In the conversion range of 0.6-0.8, with the degradation of lignin, the volatiles start diffusing within the biomass sample. The path followed by the experimental reaction model is found to vary with different conversion values. In light of this, it can be said that the pyrolysis of biomass follows a complex reaction mechanism that is impacted by the presence of hemicellulose, cellulose, and lignin in the feedstock. Therefore, the behavior of these constituents must be taken into consideration during the decomposition of biomass. It is evident that nucleation and diffusion are the mechanisms involved in the primary decomposition of hemicellulose. The DTG profile shows that maximum decomposition of hemicellulose and cellulose constituents occurs in the active pyrolytic stage (200-500 °C). In the active pyrolytic zone, from the master plot, it is identified that for conversion values 0.2 to 0.5, the reaction mechanism follows the diffusional and nucleation models. It is identified that, through the nucleation mechanism, the biomass cellulose decomposes by the formation of nuclei [66]. From the above patterns of reaction mechanisms, it is identified that the major decomposition mechanism for pyrolysis of SM seed shell biomass is nucleation followed by diffusion.

CONCLUSION

The feasibility of utilizing SM seed shell in the pyrolysis process for conversion into value added products was corroborated through proximate analysis, ultimate analysis, and calorific value. The proximate analysis shows that the SM seed shell has 68.5 % volatile matter, 1.1% ash, 9.5% moisture, and 20.9% fixed carbon. The heating value determined using the bomb calorimeter is found to be 16.06 MJ/kg. The study ascertained the pyrolysis behavior of the SM seed shell by determining its kinetic triplets and thermodynamic parameters through isoconversional model free methods (Freidman, FWO, and KAS). The average activation energies of the SM seed shell were determined as 138.14 kJ mol^{-1} for the KAS method, 140.05 kJ mol^{-1} for the OFW method, and 152.28 kJ mol^{-1} for the Friedman method. During lignin degradation, the activation energy requirement is observed to be higher than that for hemicellulose and cellulose degradation. In thermodynamic analysis, the frequency factor varied with the fractional conversion value from 0.026×10^{3} to 1.085×10^{15} s^{-1}. The average values of the thermodynamic parameters ΔH, ΔG, and ΔS determined considering the Friedman method are 148.149 kJ mol^{-1}, 157.664 kJ mol^{-1} and -0.129 kJ mol^{-1} K^{-1}, respectively. The Thermodynamic parameters showed that the pyrolysis or thermal conversion of SM seed shell is a non-spontaneous and endothermic process. The master plot shows that, SM seed shell biomass follows different degradation mechanisms such as diffusional and nucleation at different conversion values. The highly porous nature of char promotes the diffusion of volatiles from biomass samples. So, at higher conversional values, the decomposition process follows the diffusional model. The nucleation model is identified as the major decomposition mechanism compared to the diffusion model. The physicochemical and kinetic characteristics of the SM seed shell clearly indicate that it can be used as a potential feedstock for the pyrolysis process and also helps in understanding the decomposition process during thermochemical conversion.

ABBREVIATIONS

SM	Sapindus mukorossi
HHV	Higher Heating Value
TGA	Thermogravimetric analysis
OFW	Ozawa-Flynn-Wall
KAS	Kissinger-Akahira Sunose
DAEM	Distributed Activation Energy Models
ASTM	American Society for Testing and Materials
DTG	Differential Thermogravimetric analysis (DTG)

AUTHOR CONTRIBUTION

All the authors equally contributed to this work.

DATA AVAILABILITY STATEMENT

The authors confirm that the data that supports the findings of this study are available within the article. Raw data that support the finding of this study are available from the corresponding author, upon reasonable request.

CONFLICT OF INTEREST

The author declared no potential conflicts of interest with respect to the research, authorship, and/or publication of this article.

ETHICS

There are no ethical issues with the publication of this manuscript.

REFERENCES

[1] Deep Singh A, Gajera B, Sarma AK. Appraising the availability of biomass residues in India and their bioenergy potential. Waste Manage 2022;152:38-47. [CrossRef]

[2] Singh NB, Kumar A, Rai S. Potential production of bioenergy from biomass in an Indian perspective. Renew Sustain Energy Rev 2014;39:65-78. [CrossRef]

[3] Tolessa A. Bioenergy production potential of available biomass residue resources in Ethiopia. J Renew Energy 2023;2023:1-12. [CrossRef]

[4] Ben Abdallah A, Ben Hassen Trabelsi A, Navarro MV, Veses A, García T, Mihoubi D. Pyrolysis of tea and coffee wastes: Effect of physicochemical properties on kinetic and thermodynamic characteristics. J Therm Anal Calorim 2023;148:2501-2515. [CrossRef]

[5] Srivastava RK, Shetti NP, Reddy KR, Nadagouda MN, Badawi M, Bonilla-Petriciolet A, et al. Valorization of biowastes for clean energy production, environmental depollution and soil fertility. J Environ Manage 2023;332. [CrossRef]

[6] Nahar Myyas R, Tostado-Véliz M, Gómez-González M, Jurado F. Review of bioenergy potential in Jordan. Energies (Basel) 2023;16:1393. [CrossRef]

[7] Poyilil S, Palatel A, Chandrasekharan M. Physicochemical characterization study of coffee husk for feasibility assessment in fluidized bed gasification process. Environ Sci Pol Res 2022;29:51041-51053. [CrossRef]

[8] Chan YH, Cheah KW, How BS, Loy ACM, Shahbaz M, Singh HKG, et al. An overview of biomass thermochemical conversion technologies in Malaysia. Sci Total Environ 2019;680:105-123. [CrossRef]

[9] Kumar G, Parvathy Eswari A, Kavitha S, Dinesh Kumar M, Kannah RY, How LC, et al. Thermochemical conversion routes of hydrogen production from organic biomass: processes, challenges and limitations. Biomass Conver Biorefin 2020;13:8509−8534. [CrossRef]

[10] Osman AI, Farghali M, Ihara I, Elgarahy AM, Ayyad A, Mehta N, et al. Materials, fuels, upgrading, economy, and life cycle assessment of the pyrolysis of algal and lignocellulosic biomass: A review. Environ Chem Lett 2023;21:1419-1476. [CrossRef]

[11] Ranganathan P, Gu S. Computational fluid dynamics modelling of biomass fast pyrolysis in fluidised bed reactors, focusing different kinetic schemes. Bioresour Technol 2016;213:333-341. [CrossRef]

[12] Alves JLF, da Silva JCG, da Silva Filho VF, Alves RF, de Araujo Galdino WV, De Sena RF. Kinetics and thermodynamics parameters evaluation of pyrolysis of invasive aquatic macrophytes to determine their bioenergy potentials. Biomass Bioenergy 2019;121:28-40. [CrossRef]

[13] Wang G, Zhang J, Zhang G, Ning X, Li X, Liu Z, et al. Experimental and kinetic studies on co-gasification of petroleum coke and biomass char blends. Energy 2017;131:27-40. [CrossRef]

[14] Zou H, Zhang J, Liu J, Buyukada M, Evrendilek F, Liang G. Pyrolytic behaviors, kinetics, decomposition mechanisms, product distributions and joint optimization of Lentinus edodes stipe. Energy Conver Manage 2020;213:112858. [CrossRef]

[15] Mujtaba M, Fernandes Fraceto L, Fazeli M, Mukherjee S, Savassa SM, Araujo de Medeiros G, et al. Lignocellulosic biomass from agricultural waste to the circular economy: a review with focus on biofuels, biocomposites and bioplastics. J Clean Prod 2023;402:136815. [CrossRef]

[16] Suhagia BN, Rathod Is, Sindhu S. Sapindus mukorossi (Areetha): An overview. IJPSR 2011;2:1905-1913.

[17] Venkatesan V, Nallusamy N, Nagapandiselvi P. Waste-to-energy approach for utilizing non-edible soapnut oil methyl ester as a fuel in a twin-cylinder agricultural tractor diesel engine. Energy Fuels 2020;34:1958-1964. [CrossRef]

[18] Rai S, Acharya-Siwakoti E, Kafle A, Devkota HP, Bhattarai A. Plant-derived saponins: A review of their surfactant properties and applications. Sci 2021;3:44. [CrossRef]

[19] Mukhopadhyay S, Mukherjee S, Hashim MA, JN S, Villegas NM, Sen Gupta B. Zinc removal from soil by washing with saponin obtained from Sapindus mukorossi. J Environ Anal Chem 2018;5:1−8. [CrossRef]

[20] Ponnam V, Ghodke P, Tondepu S, Mandapati RN. Thermal behaviour kinetic modeling of capsicum annuum waste biomass using an iso-conversion method. J Themr Engineer 2021;7:18−29. [CrossRef]

[21] Agnihotri N, Mondal MK. Thermal analysis, kinetic behavior, reaction modeling, and comprehensive pyrolysis index of soybean stalk pyrolysis. Biomass Conver Biorefin 2024;14:14977-14992. [CrossRef]

[22] Atkins P, de Paula J. Physical Chemistry. New York: W. H. Freeman and Company; 2006.

[23] Jagtap A, Kalbande SR. Investigation on pyrolysis kinetics and thermodynamic parameters of soybean straw: A comparative study using model-free methods. Biomass Conver Biorefin 2022;02228-9. [CrossRef]

[24] Mishra A, Nanda S, Ranjan Parida M, Jena PK, Dwibedi SK, Manjari Samantaray S, et al. A comparative study on pyrolysis kinetics and thermodynamic parameters of little millet and sunflower stems biomass using thermogravimetric analysis. Bioresour Technol 2023;367:128231. [CrossRef]

[25] Vyazovkin, Sergey CAW. Model-free and model-®t-ting approaches to kinetic analysis of isothermal and nonisothermal data. Thermochim Acta 1999;340-341:53-68. [CrossRef]

[26] Junges J, Silvestre WP, De Conto D, Baldasso C, Osório E, Godinho M. Non-isothermal kinetic study of fodder radish seed cake pyrolysis: performance of model-free and model-fitting methods. Braz J Chem Engineer 2020;37:139-155. [CrossRef]

[27] Mishra RK, Mohanty K. Pyrolysis kinetics and thermal behavior of waste sawdust biomass using thermogravimetric analysis. Bioresour Technol 2018;251:63-74. [CrossRef]

[28] Patnaik S, Panda AK, Kumar S. Thermal degradation of corn starch based biodegradable plastic plates and determination of kinetic parameters by isoconversional methods using thermogravimetric analyzer. J Energy Inst 2020;93:1449-1459. [CrossRef]

[29] Vasudev V, Ku X, Lin J. Pyrolysis of algal biomass: Determination of the kinetic triplet and thermodynamic analysis. Bioresour Technol 2020;317:124007. [CrossRef]

[30] Barr MR, Volpe M, Messineo A, Volpe R. On the suitability of thermogravimetric balances for the study of biomass pyrolysis. Fuel 2020;276:118069. [CrossRef]

[31] Rajamohan S, Chidambaresh S, Sundarrajan H, Balakrishnan S, Sirohi R, Cao DN, et al. Investigation of thermodynamic and kinetic parameters of Albizia lebbeck seed pods using thermogravimetric analysis. Bioresour Technol 2023;384:129333. [CrossRef]

[32] Broström M, Nordin A, Pommer L, Branca C, Di Blasi C. Influence of torrefaction on the devolatilization and oxidation kinetics of wood. J Anal Appl Pyrolysis 2012;96:100-109. [CrossRef]

[33] Tapasvi D, Khalil R, Várhegyi G, Tran KQ, Grønli M, Skreiberg Ø. Thermal decomposition kinetics of woods with an emphasis on torrefaction. Energy Fuels 2013;27:6134-6145. [CrossRef]

[34] Vyazovkin S, Burnham AK, Criado JM, Pérez-Maqueda LA, Popescu C, Sbirrazzuoli N. ICTAC Kinetics Committee recommendations for performing kinetic computations on thermal analysis data. Thermochim Acta 2011;520:1-19. [CrossRef]

[35] Vyazovkin S, Chrissafis K, Di Lorenzo ML, Koga N, Pijolat M, Roduit B, et al. ICTAC Kinetics Committee recommendations for collecting experimental thermal analysis data for kinetic computations. Thermochim Acta 2014;590:1-23. [CrossRef]

[36] Yang Z, Zhang L, Zhang Y, Bai M, Zhang Y, Yue Z, et al. Effects of apparent activation energy in pyrolytic carbonization on the synthesis of MOFs-carbon involving thermal analysis kinetics and decomposition mechanism. Chem Engineer J 2020;395:124980. [CrossRef]

[37] Ahmad MS, Klemeš JJ, Alhumade H, Elkamel A, Mahmood A, Shen B, et al. Thermo-kinetic study to elucidate the bioenergy potential of Maple Leaf Waste (MLW) by pyrolysis, TGA and kinetic modelling. Fuel 2021;293:120349. [CrossRef]

[38] Pal DB, Tiwari AK, Prasad N, Srivastava N, Almalki AH, Haque S, et al. Thermo-chemical potential of solid waste seed biomass obtained from plant Phoenix dactylifera and Aegle marmelos L. Fruit core cell. Bioresour Technol 2022;345:126441. [CrossRef]

[39] Komandur J, Vinu R, Mohanty K. Pyrolysis kinetics and pyrolysate composition analysis of Mesua ferrea L: A non-edible oilseed towards the production of sustainable renewable fuel. Bioresour Technol 2022;351:126987. [CrossRef]

[40] Żółtowska S, Koltsov I, Alejski K, Ehrlich H, Ciałkowski M, Jesionowski T. Thermal decomposition behaviour and numerical fitting for the pyrolysis kinetics of 3D spongin-based scaffolds. The classic approach. Polym Test 2021;97:107148. [CrossRef]

[41] Singh RK, Patil T, Sawarkar AN. Pyrolysis of garlic husk biomass: Physico-chemical characterization, thermodynamic and kinetic analyses. Bioresour Technol Rep 2020;12;100558. [CrossRef]

[42] He Q, Ding L, Gong Y, Li W, Wei J, Yu G. Effect of torrefaction on pinewood pyrolysis kinetics and thermal behavior using thermogravimetric analysis. Bioresour Technol 2019;280:104-111. [CrossRef]

[43] Cai H, Liu J, Xie W, Kuo J, Buyukada M, Evrendilek F. Pyrolytic kinetics, reaction mechanisms and products of waste tea via TG-FTIR and Py-GC/MS. Energy Conver Manage 2019;184:436-447. [CrossRef]

[44] Luo L, Zhang Z, Li C, Nishu, He F, Zhang X, et al. Insight into master plots method for kinetic analysis of lignocellulosic biomass pyrolysis. Energy 2021;233:121194. [CrossRef]

[45] Upadhyay A, Singh DK. Pharmacological effects of Sapindus mukorossi. Rev Inst Med Trop Sao Paulo 2012;54:273-80. [CrossRef]

[46] Mishra RK, Mohanty K. Pyrolysis of Cascabela thevetia seeds over ZSM-5 catalysts: Fuel properties and compositional analysis. Biomass Conver Biorefin 2022;12:1449-1464. [CrossRef]

[47] Khawam A, Flanagan DR. Solid-state kinetic models: Basics and mathematical fundamentals. J Physical Chem B 2006;110:17315-17328. [CrossRef]

[48] Mishra RK, Mohanty K. Kinetic analysis and pyrolysis behaviour of waste biomass towards its bioenergy potential. Bioresour Technol 2020;311:123480. [CrossRef]

[49] Kaur R, Gera P, Jha MK, Bhaskar T. Pyrolysis kinetics and thermodynamic parameters of castor (Ricinus communis) residue using thermogravimetric analysis. Bioresour Technol 2018;250:422-428. [CrossRef]
[50] Criado JM, Málek J, Ortega A. Applicability of the master plots in kinetic analysis of non-isothermal data. Thermochim Acta 1989;147:377-385. [CrossRef]
[51] Li Y, Cheng Y, Ye Y, Shen R. Supplement on applicability of the Kissinger equation in thermal analysis. J Therm Anal Calorim 2010;102:605-608. [CrossRef]
[52] Sahoo A, Kumar S, Mohanty K. Kinetic and thermodynamic analysis of Putranjiva roxburghii (putranjiva) and Cassia fistula (amaltas) non-edible oilseeds using thermogravimetric analyzer. Renew Energy 2021;165:261-277. [CrossRef]
[53] Shadangi KP, Mohanty K. Comparison of yield and fuel properties of thermal and catalytic Mahua seed pyrolytic oil. Fuel 2014;117:372-380. [CrossRef]
[54] Karaeva JV, Timofeeva SS, Islamova SI, Gerasimov AV. Pyrolysis kinetics of new bioenergy feedstock from anaerobic digestate of agro-waste by thermogravimetric analysis. J Environ Chem Engineer 2022;10:107850. [CrossRef]
[55] Silva JE, Calixto GQ, de Almeida CC, Melo DMA, Melo MAF, Freitas JCO, et al. Energy potential and thermogravimetric study of pyrolysis kinetics of biomass wastes. J Therm Anal Calorim 2019;137:1635-1643. [CrossRef]
[56] Gai C, Zhang Y, Chen WT, Zhang P, Dong Y. Thermogravimetric and kinetic analysis of thermal decomposition characteristics of low-lipid microalgae. Bioresour Technol 2013;150:139-148. [CrossRef]
[57] Morais LC, Maia AAD, Guandique MEG, Rosa AH. Pyrolysis and combustion of sugarcane bagasse. J Therm Anal Calorim 2017;129:1813-1822. [CrossRef]
[58] Biagini E, Fantei A, Tognotti L. Effect of the heating rate on the devolatilization of biomass residues. Thermochim Acta 2008;472:55-63. [CrossRef]
[59] Gogoi M, Konwar K, Bhuyan N, Borah RC, Kalita AC, Nath HP, et al. Assessments of pyrolysis kinetics and mechanisms of biomass residues using thermogravimetry. Bioresour Technol Rep 2018;4:40-49. [CrossRef]
[60] Wang S, Lin H, Ru B, Dai G, Wang X, Xiao G, et al. Kinetic modeling of biomass components pyrolysis using a sequential and coupling method. Fuel 2016;185:763-771. [CrossRef]
[61] Vyazovkin S, Burnham AK, Favergeon L, Koga N, Moukhina E, Pérez-Maqueda LA, et al. ICTAC Kinetics Committee recommendations for analysis of multi-step kinetics. Thermochim Acta 2020;689:178597. [CrossRef]
[62] Cai J, Xu D, Dong Z, Yu X, Yang Y, Banks SW, et al. Processing thermogravimetric analysis data for isoconversional kinetic analysis of lignocellulosic biomass pyrolysis: Case study of corn stalk. Renew Sustain Energy Rev 2018;82:2705-2715. [CrossRef]
[63] Turmanova SC, Genieva SD, Dimitrova AS, Vlaev LT. Non-isothermal degradation kinetics of filled with rise husk ash polypropene composites. Express Polym Lett 2008;2:133-146. [CrossRef]
[64] Ali I, Bahaitham H, Naibulharam R. A comprehensive kinetics study of coconut shell waste pyrolysis. Bioresour Technol 2017;235:1-11. [CrossRef]
[65] Gu T, Fu Z, Berning T, Li X, Yin C. A simplified kinetic model based on a universal description for solid fuels pyrolysis: Theoretical derivation, experimental validation, and application demonstration. Energy 2021;225:120133. [CrossRef]
[66] Burnham AK, Zhou X, Broadbelt LJ. Critical review of the global chemical kinetics of cellulose thermal decomposition. Energy Fuels 2015;29:2906-2918. [CrossRef]